Journal of Power Sources 257 (2014) 286–292

Contents lists available at ScienceDirect

Journal of Power Sources

journal homepage: www.elsevier.com/locate/jpowsour

Impact of active material surface area on thermal stability of $LiCoO_2$ cathode

Jan Geder [a,*], Harry E. Hoster [a], Andreas Jossen [b], Jürgen Garche [c], Denis Y.W. Yu [a,d]

[a] TUM CREATE Limited, Singapore
[b] Institute for Electrical Energy Storage Technology at Technische, Universität München, Germany
[c] Fuel Cell and Battery Consulting – FCBAT Ulm, Germany
[d] School of Energy and Environment, City University of Hong Kong, Hong Kong Special Administrative Region

HIGHLIGHTS

- Higher surface area of $LiCoO_2$ significantly reduces thermal stability of cathodes.
- High surface area changes $LiCoO_2$ decomposition reaction mechanism.
- Activation energy of cathode decomposition decreases with increasing surface area.
- Cathodes with high surface area $LiCoO_2$ react more exothermally with the electrolyte.
- Ball milling is not advisable method for treatment of $LiCoO_2$.

ARTICLE INFO

Article history:
Received 28 November 2013
Received in revised form
28 January 2014
Accepted 31 January 2014
Available online 10 February 2014

Keywords:
Lithium-ion battery
Cathode
$LiCoO_2$
Thermal stability
Thermal analysis

ABSTRACT

Thermal stability of charged $LiCoO_2$ cathodes with various surface areas of active material is investigated in order to quantify the effect of $LiCoO_2$ surface area on thermal stability of cathode. Thermogravimetric analyses and calorimetry have been conducted on charged cathodes with different active material surface areas. Besides reduced thermal stability, high surface area also changes the active material decomposition reaction and induces side reactions with additives. Thermal analyses of $LiCoO_2$ delithiated chemically without any additives or with a single additive have been conducted to elaborate the effect of particle size on side reactions. Stability of cathode–electrolyte system has been investigated by accelerating rate calorimetry (ARC). Arrhenius activation energy of cathode decomposition has been calculated as function of conversion at different surface area of active material.

1. Introduction

$LiCoO_2$ has been used extensively as active material for cathodes in Li-ion batteries. Due to its good balance between capacity, safety and ease of processing (as compared to other cathode materials) [1], it is still the most common active material in cathodes at least for consumer lithium ion cells.

One of the main issues concerning the lithium-ion battery technology is its low power density [2], which is limited by the movement of Li ions in the active material. Ionic diffusion path can be reduced by using cathode active materials with smaller particle size to enhance rate capability and power density. There have been many efforts lately to use nano-sized $LiCoO_2$ as cathode material for high-power applications [3,4]. However, smaller particle size translates to higher surface area, which leads to higher irreversible capacity loss due to side reactions and faster ageing of battery cells [5]. Nevertheless, an optimal particle size in terms of performance is believed to exist in the submicron particle size range for $LiCoO_2$ [3].

Possible effects on thermal stability are another concern for the high surface area active material. Charged $Li_{1-x}CoO_2$ cathode is known to decompose at elevated temperatures or higher voltages. The decomposition reaction yields oxygen, which can react exothermally with the organic electrolyte or cathode additives, leading to thermal runaway of the battery cell. Higher surface area increases the probability of surface reactions, which jeopardises the stability of the cathode as well as of cathode–electrolyte system.

* Corresponding author.
E-mail addresses: jan.geder@tum-create.edu.sg (J. Geder), denisyu@cityu.edu.hk (D.Y.W. Yu).

http://dx.doi.org/10.1016/j.jpowsour.2014.01.116
0378-7753/

Decomposition mechanism of $Li_{1-x}CoO_2$ was reported [6,7] to yield $LiCoO_2$, Co_3O_4 and O_2, according to equation (1) below.

$$Li_{1-x}CoO_2 \rightarrow (1-x)LiCoO_2 + \frac{x}{3}Co_3O_4 + \frac{x}{3}O_2 \quad (1)$$

Cobalt (II,III) oxide, formed in above suggested decomposition can further react with conductive carbon additive.

$$Co_3O_4 + \frac{1}{2}C \rightarrow 3CoO + \frac{1}{2}CO_2 \quad (2)$$

At higher temperatures (>900 °C) or in presence of organic electrolyte, CoO can be further reduced to Co [8]. Both reactions (1) and (2) are exothermal. Released heat can increase the temperature up to the ignition point of liquid electrolyte, typically an organic carbonate. Furthermore, the polymer binder can decompose either by reacting with oxygen from decomposition reaction (1) or anaerobically, adding another exothermal reaction to the process of cathode decomposition.

While there is much research focussing on performance-related effects of particle size and surface area of $LiCoO_2$ [3,4,9] as well as other cathode and anode materials [2,5], the amount of research focussing on thermal stability effects of particle size is rather scarce [8].

Jiang and Dahn [8] have found a clear link between $LiCoO_2$ particle size and thermal stability of cathode-electrolyte system using accelerating rate calorimetry (ARC). As expected, the onset temperature of the reaction between cathode and electrolyte is lower for small particles. Also, the self-heating rate of the reactive system is higher and increases faster for smaller particles.

The purpose of this article is to elucidate the relationship between the particle sizes of $LiCoO_2$ and thermal stability of cathode itself as well as cathode-electrolyte system. High surface area can facilitate the decomposition reaction (1) due to reduced thermodynamic stability of smaller particles. Faster reaction kinetics due to higher surface area and consequentially faster oxygen release is also possible. Furthermore, it is suspected that higher surface area could catalyse the side reactions with additives and reduction of cobalt (II,III) oxide.

In order to investigate kinetics of decomposition reactions in charged $LiCoO_2$ cathodes, the method of non-isothermal model-free kinetic analysis of the thermogravimetric data can be applied, also known as the Friedman-Ozawa method. The method [10,11] is based on the assumption that the rate of the reaction, which equals the derivative of conversion (α) over time, can be expressed as a product of two functions. The first function depends only on temperature ($k(T)$) and the second depends only on conversion itself ($f(\alpha)$). In case of thermogravimetric analysis (TGA), conversion of a decomposition reaction is directly proportional to the relative mass loss.

$$\frac{d\alpha}{dt} = k(T)\cdot f(\alpha) \quad (3)$$

By assuming Arrhenius law for temperature-dependent contribution to rate and replacing time by quotient of temperature and heating rate (β), equation (3) can be rearranged to

$$\beta\cdot\frac{d\alpha}{dT} = k_0 \exp\left(-\frac{E_a}{RT}\right) f(\alpha) \quad (4)$$

where E_a is the apparent activation energy of the reaction. In logarithmic form, equation (4) can be written as

$$\ln\left(\beta\frac{d\alpha}{dT}\right) = -\frac{E_a}{R}\frac{1}{T} + \ln(k_0 f(\alpha)) \quad (5)$$

At a constant value of conversion, the logarithm of the product between heating rate and derivative of conversion over temperature is directly proportional to inverse value of temperature. Thus, the activation energy can be calculated from a set of three or more TGA experiments with different heating rate at any fixed value of conversion. This method has already been applied to study the decomposition of pure, chemically de-lithiated $Li_{1-x}CoO_2$ [6]. It will be applied now to the decomposition of the cathodes with various active material surface areas.

2. Experimental

2.1. Surface area variation by ball milling

Commercial electrode-grade $LiCoO_2$ powder with average particle size of approximately 2 μm and surface area of 0.4 $m^2\ g^{-1}$ was obtained from ENAX, Japan. Batches of material with different surface area were obtained by ball milling in FRITSCH Pulverisette planetary ball mill. 2 g of $LiCoO_2$ was processed in each batch, using 15 ml acetone as liquid medium. Milling was carried out in 15 min intervals, followed by 15 min pause. Other ball milling conditions are listed in Table 1. Excessive milling may degrade the material and reduce the lithium ion diffusion [12], therefore maximum milling time was limited to 7 h. After milling, material was dried at 70 °C in vacuum. Flakes of dried material are grinded shortly in a coffee mill to obtain powder. Surface area of powders was determined by multiple-point BET adsorption method in Quantachrome Instruments NOVA sorption analyser.

Samples have been analysed by X-ray diffraction spectrometry (XRD, Bruker D8 Powder) after milling to ensure phase purity of the product.

2.2. Cathode coating, cell assembly/disassembly and formation

Slurry for cathode coating was prepared from 80% $LiCoO_2$, 10% acetylene black (AB; 50% compressed 99.9% metals basis, Alfa Aesar) and 10% polyvinylidene difluoride (PVDF; HSV900, Kynar) as 6% solution in N-Methyl-2-pyrrolidone (NMP; ACS reagent ≥99.0%, Sigma–Aldrich). This was coated on a 15 μm thick aluminium foil and dried on a hotplate at 80 °C for 3 h. Rectangular cathodes (23 by 18 mm) were cut out and pressed several times in a roll press to obtain a net electrode thickness of approximately 35 μm. The electrodes were then dried at 110 °C for 12 h in vacuum to remove any adsorbed water. Afterwards they were transferred into an argon-filled glovebox and built into pouch cells with pure metallic lithium as anode and 1 M $LiPF_6$ in EC/DEC = 1:1 (DANVEC, China) as electrolyte. A tri-layer polypropylene/polyethylene/polypropylene Cellgard 2320 separator by Cellgard, USA was used.

Each cell was initially charged, discharged and then charged again to the target composition of $Li_{0.5}CoO_2$. In the first cycle, the cell was charged with a current of 13.69 mA per gram $LiCoO_2$ (equivalent of 0.1 C) up to 4.2 V, and then held at 4.2 V until the

Table 1
Milling parameters and surface area of milled $LiCoO_2$.

Time	Rotational speed/rpm	Milling balls	Balls/$LiCoO_2$ weight ratio	Surface area/$m^2\ g^{-1}$
0 h (Pristine)	/	/	/	0.4
1 h	500	5 mm stainless steel	15:1	4.6
2 h				14.4
3 h				16.0
5 h				18.3
7 h	750	5 mm tungsten carbide	30:1	42.4

current dropped to 10% of initial value. After charging, the cell was discharged with a current of 13.69 mA g^{-1} until the voltage of 3.0 V was reached. In the next step, the cell was charged with 13.69 mA g^{-1} to a cumulative capacity of 136.9 mAh g^{-1}, equivalent to $Li_{0.5}CoO_2$. Assumption is made that no side reactions such as electrolyte decomposition take place and therefore all charge transfer quantitatively corresponds to lithium transfer from and into cathode.

Charged cells were then disassembled under inert (Ar) atmosphere. The cathodes were taken out and thoroughly washed with dimethyl carbonate (anhydrous ≥99.9%, Sigma Aldrich) and dried overnight in deep vacuum at room temperature. Coating has been scratched off the aluminium current collector for subsequent thermal analyses. These samples contain active material, carbon and binder in them.

2.3. Chemical de-lithiation of $LiCoO_2$

For comparison, $Li_{0.5}CoO_2$ powder chemically delithiated without any carbon and binder were also made with the same active materials with different surface areas to identify the effect of the electrode additives. $LiCoO_2$ was dispersed in stoichiometric amount of 0.15 M aqueous solution of potassium persulfate ($K_2S_2O_8$ > 99.0%, Sigma–Aldrich). Suspension was kept at 55 °C and stirred for 72 h. De-lithiation can be written as:

$$LiCoO_2 + \frac{x}{2}K_2S_2O_8 \rightarrow Li_{1-x}CoO_2 + \frac{x}{2}K_2SO_4 + \frac{x}{2}Li_2SO_4 \quad (6)$$

After 72 h, liquid phase has been removed by filtration and solid remaining has been extensively washed with de-ionized water at 55 °C. The product has been dried in vacuum for an additional 72 h.

2.4. Thermal analysis and mass spectrometry

For thermal analysis, samples were sealed into 100 μl aluminium crucibles with lid by cold welding. Sample can be either charged dried cathode or chemically delithiated $Li_{0.5}CoO_2$ with or without additives. Thermogravimetric analysis (TGA) was performed under argon flow of 30 ml min^{-1} by Mettler Toledo STARe TGA/DSC1 thermal analyser. A small hole has been poked into the lid of the sealed crucible by sampling robot prior to analysis to allow the evolved gases to escape.

In the first series of screening experiments, electrochemically charged and dried cathodes made of all batches of $LiCoO_2$ listed in Table 1 have been heated up at 5 K min^{-1} to 400 °C and held at this temperature for 1 h. The final temperature was chosen to be below the decomposition temperature of PVDF, which is estimated at 470 °C [13]. Afterwards, pristine $LiCoO_2$, and the $LiCoO_2$ milled for 5 and 7 h, have been delithiated chemically as described in 2.3 and analysed under the same heating rate and gas flow up to 600 °C. Same analyses were also done for these three batches of $LiCoO_2$ chemically delithiated with addition of either AB or PVDF in weight ratio of 1:8 to study the differences.

For the cathodes made of selected materials in the above paragraph, TGA has been repeated at changing rates of 5, 10, 15 and 20 K min^{-1} in interval between 25 °C and 600 °C.

2.5. Accelerating rate calorimetry

For ARC analysis, charged cathode from a pouch cell has been washed with DMC, dried and cut to a circle with a diameter of 16 mm. It was sealed in the casing of 2016 coin cell (without gasket) together with electrolyte in mass ratio 2:1 (cathode:electrolyte). The sample was strapped to the thermocouple of ARC in horizontal position and analysed according to the standard heat-wait-search procedure [14]. Sample-containing cell was heated to initial temperature of 100 °C. A waiting period of 20 min was set for system to reach thermal equilibrium. After that, the calorimeter sought for any possible exothermal effect (self-heating) for 10 min at sensitivity of 0.02 K min^{-1}. If self-heating occurs, the system responds by tracking the temperature. If not, the system heats up the sample by 3 °C and repeats the procedure.

3. Results and discussion

3.1. Cell assembly and electrochemical characterization

Table 1 shows detailed milling parameters for each batch and surface area of the products.

Fig. 1 shows selected SEM images of pristine and ball-milled $LiCoO_2$. Ball milling yields considerably smaller particles of irregular shape with inhomogeneous particle size distribution. Considering the irregularly shaped structure of the particles, certain extent of surface damage imposed by ball milling cannot be completely excluded. Due to the very broad particle size distribution, some particle appear to be nano-sized, rather than submicron.

Fig. 2 shows XRD spectra of pristine and milled samples, compared to reference spectrum of layered $LiCoO_2$. Peak positions reveal that ball milling does not change the phase composition of the material. However, peak broadening can be seen after extended milling. Crystallinity of $LiCoO_2$ is therefore reduced even at shorter exposure times than reported by Nakamura et al. [12], who used similar type of mill with zirconia balls. The milled samples also show increasing changes in peak ratios, which may be due to cation mixing in the material induced by the milling process.

First cycle and subsequent charging of the cathodes is shown on Fig. 3. Charge capacity of the cathodes in first cycle varies significantly with changing surface area, yet no trend related to surface area can be seen. However, first cycle curves are not representative since some balancing processes in the cathode/active material may not be completed. Discharge capacity is lower for cathodes with higher $LiCoO_2$ surface area. As a consequence, the first cycle irreversible capacity loss is higher for materials with higher surface area. One reason for this is insufficient contact between irregularly shaped or small particles in high-surface cathodes with acetylene black. Also, long exposure to milling incurs certain damage to surface. This then affects mobility of Li ions. Charge profiles of the cathodes with milled $LiCoO_2$ have slower voltage increase in the beginning. During the second charge, the voltage profiles of cathodes with milled LiCoO2 appear to be lower. Okubo et al. [15] found similar behaviour for nano-crystalline $LiCoO_2$ and suggested grain size to be cause of this phenomenon.

3.2. Thermal stability of cathodes

All test cells were charged to an accumulative capacity of 136.9 mAh g^{-1} ($Li_{0.5}CoO_2$). The cells were disassembled, washed and dried, followed by TGA tests. Fig. 4 shows the TGA curves of dried charged cathodes with different surface area of $LiCoO_2$. It can be clearly seen that higher surface area reduces thermal stability by reducing onset temperature of decomposition and increasing the total mass loss. For pristine $LiCoO_2$ particles, the total mass loss is about 5% when tested to 400 °C, which is consistent with the 4.49% theoretical mass loss due to oxygen loss according to equation (1) for a cathode with 80% $LiCoO_2$. Overall mass loss at the end of temperature program increases almost linearly with surface area, as shown on Fig. 5. The cause of increasing mass loss at higher $LiCoO_2$ surface area could suggest either increased amount of

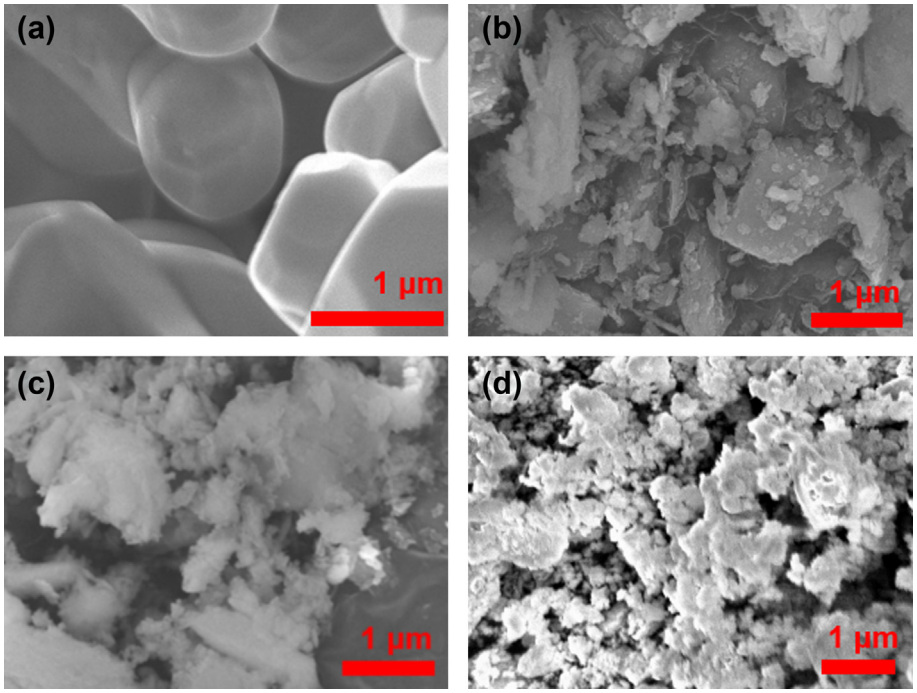

Fig. 1. SEM images of $LiCoO_2$: pristine material (a), milled material with 16.0 $m^2\ g^{-1}$ (b), milled material with 18.3 $m^2\ g^{-1}$ (c) and milled material with 42.4 $m^2\ g^{-1}$ (d).

decomposition from the additives in the electrode, or a change in decomposition mechanism of $LiCoO_2$. Maximum theoretical mass loss of the cathode with given composition is estimated at 19.55%, under assumption that all cobalt oxide is reduced to CoO, all thereby released oxygen reacts with carbon, and PVDF completely decomposes anaerobically. This value is not reached by any of the samples during the temperature program. The role of the carbon and binder additives is evaluated in the next section to clarify the reason for the observed mass loss.

3.3. Role of active material and additives in decomposition

To understand the reaction process of the electrode material during the thermal decomposition, thermal analysis has been repeated on chemically delithiated selected materials to isolate the effects of the additives. Fig. 6 shows TGA curves for pure chemically

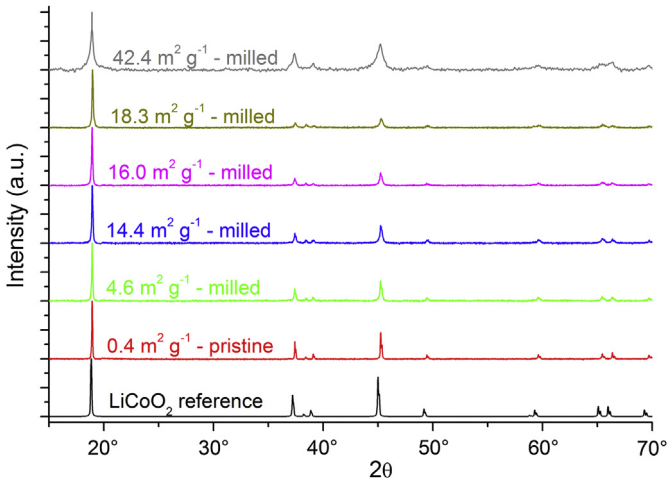

Fig. 2. XRD of pristine and ball-milled $LiCoO_2$ compared to reference spectrum.

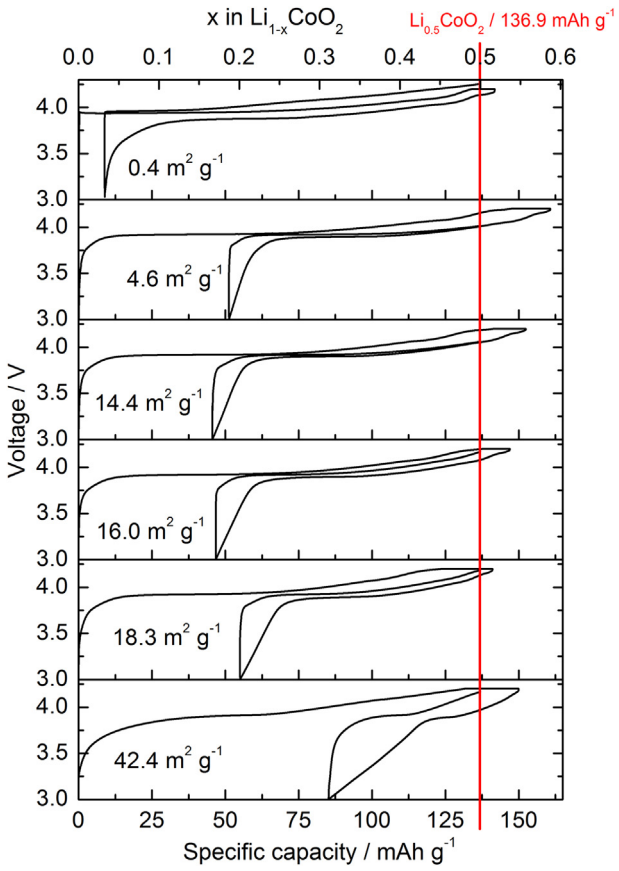

Fig. 3. Voltage profiles of cells with different batches of $LiCoO_2$ as cathode material and Li metal as anode during first charge–discharge cycle and subsequent charge. Cumulative capacity was limited to 136.9 mAh g^{-1} (equivalent to $Li_{0.5}CoO_2$) during the second (last) charge step.

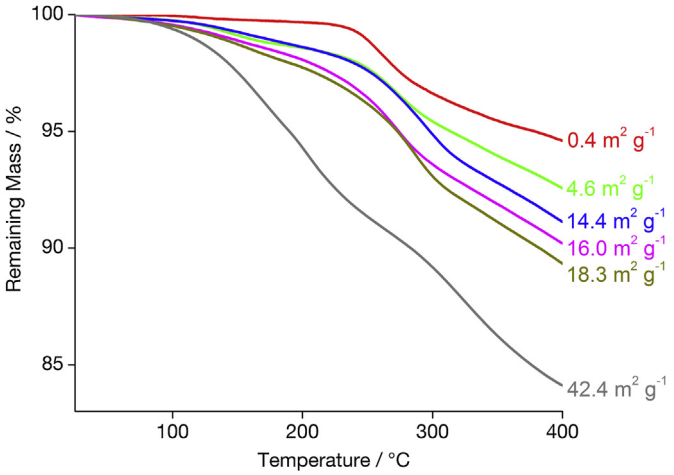

Fig. 4. TGA of charged cathodes under 30 ml min^{-1} argon flow and a heating rate of 5 K min^{-1}.

de-lithiated $Li_{0.5}CoO_2$ powder with or without AB and PVDF additives, as well as electrochemically charged $Li_{0.5}CoO_2$ electrodes. Curves are normalized to amount of active material.

Table 2 summarizes the data from Fig. 6.

Chemically delithiated pristine (0.4 m^2 g^{-1}) sample shows a total mass loss of 4.30% at 600 °C, which is below the theoretical value according to equation (1). Mixing with acetylene black increases overall mass loss beyond 500 °C. Mixing with PVDF shows a mass drop at 470 °C, which corresponds to the decomposition temperature of PVDF. When the surface area is increased to 18.3 m^2 g^{-1} and 42.4 m^2 g^{-1}, the corresponding mass loss for the chemically delithiated powder without additives are 8.10% and 13.84%, respectively. This is higher than the theoretical maximum of 5.45 according to equation (1). Presence of acetylene black adds 2.90, 3.09 and 2.56 percentage points to mass loss for 0.4, 18.3 and 42.4 m^2 g^{-1} $Li_{0.5}CoO_2$, respectively. Presence of PVDF adds 11.97, 11.69 and 6.72 percentage points to mass loss for 0.4, 18.3 and 42.4 m^2 g^{-1} $Li_{0.5}CoO_2$, respectively.

Therefore, amount of additives reacted in side reaction seems to vary among the $LiCoO_2$ samples with different surface area; however no clear trend can be seen from the three observed $LiCoO_2$ samples. Clearly, higher surface area does not catalyse side reaction between additives and active material. Amount of reacted/decomposed additives is more likely to depend on availability of O_2 in the temperature range of decomposition/combustion. The major part of the difference in mass loss between cathodes with different surface area comes from the active material itself. Mass loss of pure chemically delithiated $LiCoO_2$ is almost doubled with increasing surface area from 0.4 to 18.3 m^2 g^{-1} and more than tripled when surface area of $LiCoO_2$ is increased 42.4 m^2 g^{-1}. For chemically delithiated $LiCoO_2$ sample with highest surface area, two stages of mass loss can be observed, one before 250 °C and one after. This is not the case for other two chemically delithiated samples.

Total amount of TGA weight loss from the cathode therefore comes from three contributions: mass loss from active material, mass loss from carbon, and mass loss from binder. The contributions are independent of each other and the most significant difference between various $LiCoO_2$ samples comes from the active material.

Above findings imply that there might be a different decomposition reaction happening for $LiCoO_2$ with different surface area. In order to elucidate the reasons behind these phenomena, XRD spectrum of cathode decomposition products after TGA was taken for the 0.4, 18.3 and 42.4 m^2 g^{-1} samples. Fig. 7 shows the XRD spectra for the decomposed cathodes (after heated to 600 °C in TGA) with $LiCoO_2$. The pristine $Li_{0.5}CoO_2$ electrode after annealing shows $LiCoO_2$, Co_3O_4 and CoO peaks, suggesting that the decomposition is according to equations (1) and (2). On the other hand, milled high-surface $LiCoO_2$ electrodes do not decompose under the same mechanism. In particular, the peaks characteristic for layered (R-3m) $LiCoO_2$ have very low intensity. The tallest peak related to layered $LiCoO_2$ around 19° (003) is almost completely absent, which indicates change in crystal structure. This suggests the formation of the Li—Co—O system with rock salt (Fm-3m) structure.

In rock salt structure, Li and Co atoms are occupying the cation sites randomly [16]. Formation of rock salt structured $Li_yCo_{2-y}O_2$ ($0 \leq y \leq 1$) can explain the absence of (003) peak in the XRD spectra of high surface area cathodes after decomposition. Unfortunately, peaks of rock salt $Li_yCo_{2-y}O_2$ overlap with peaks of CoO, which also crystallizes in Fm-3m space group. Furthermore, changed ratio between atoms in rock salt Li—Co—O system explains partly the increased mass loss at decomposition. Assumed that rock salt $Li_yCo_{2-y}O_2$ with $y = 0.8$ completely replaced layered $LiCoO_2$ as decomposition product according to equation (1), the reaction equation changes to:

$$Li_{0.5}CoO_2 \rightarrow \frac{5}{8}Li_{0.8}Co_{1.2}O_2 + \frac{1}{12}Co_3O_4 + \frac{5}{24}O_2 \quad (7)$$

Theoretical mass loss according to equation (7) exceeds 7%. In case that CoO is also formed during decomposition, the mass loss can be even higher, up to 8.4%. Lower values of y in $Li_yCo_{2-y}O_2$ further decrease the theoretical mass loss. Nevertheless, presence of Co_3O_4 in XRD pattern of decomposition products ($2\theta = 31°$) implies that there is a stoichiometric limit at $y = 0.66$.

Linear relationship between surface area and mass loss (Fig. 5) implies that there may be two different reactions occurring in the bulk and at the surface of $LiCoO_2$, where the surface reaction contributes to higher mass loss. If the surface of smaller particles is not stable, it releases more oxygen and the rock-salt structure becomes a stable phase with oxygen deficiency on the surface.

Formation of rock salt phase may as well be related to structural/surface defects caused by ball milling. It was shown in the literature [18] that during mechano-chemical synthesis of $LiCoO_2$, rock salt phase is formed during prolonged milling. This should be, however, not the case in the present work, since the presence of rock salt phase is not seen in any of the $LiCoO_2$ samples after milling (Fig. 2). Nevertheless, milling induced defects are not completely to exclude.

Further research is required to prove the hypothesis of rock salt structure formation.

3.4. Kinetics of cathode decomposition

Fig. 8 shows Arrhenius activation energy calculated according to equation (5) as a function of decomposed mass fraction of the 0.4, 18.3 and 42.4 m^2 g^{-1} charged cathodes. Relatively narrow error bars for most of the points indicate that experimental data fit well to the Friedman-Ozawa model. Clearly, at lower conversion values, the apparent activation energy is lower for the cathodes with higher $LiCoO_2$ surface area.

The activation energy rises with conversion, which is attributed to lower concentration of active reactant, parts of which are converted to $LiCoO_2$, Co_3O_4 and O_2. Also, rising trend of activation energy versus conversion indicates occurrence of competitive reactions [11]. This can be related either to reaction (2) or to combustion and decomposition of additives. For pristine $LiCoO_2$ with the lowest surface area of 0.4 m^2 g^{-1}, activation energy reaches its maximum after approximately 2.5% of total mass is decomposed.

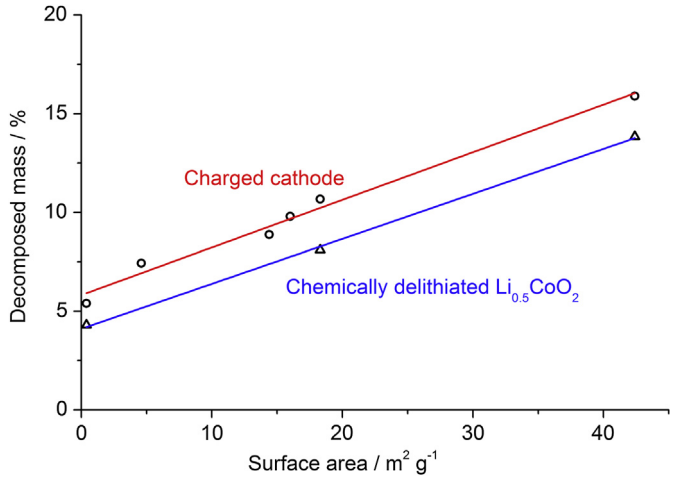

Fig. 5. Decomposed mass fraction of cathode at 400 °C. Linear relationship with surface area is observed ($R^2 = 0.982$). Linear trend is also visible for chemically delithiated $Li_{0.5}CoO_2$ at 400 °C.

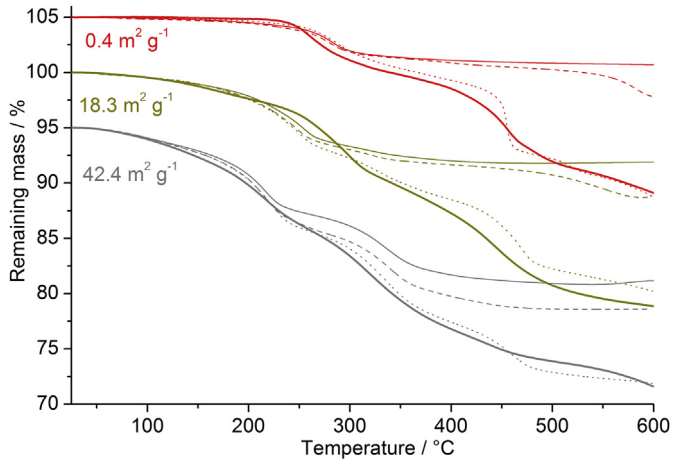

Fig. 6. TGA of chemically delithiated $Li_{0.5}CoO_2$: alone (thin line), with acetylene black (dashed line), with PVdF (dotted line). Results are compared with TGA of charged cathodes (thick line). Heating rate 5 K min^{-1}, argon flow 30 ml min^{-1}. Curves are shifted 5% vertically for clarity purpose. Curves are normalized to amount of active material in order to be comparable.

This can be indicating the point where side reactions, such as oxidation or decomposition of additives, take over the dominant role in cathode decomposition reaction. High surface area (18.3 and 42.4 m^2 g^{-1}) cathodes do not reach this turning point in the observed interval of conversion (up to 4% decomposed mass), since more of the active material decomposes before the side reactions become dominant.

Lower (apparent) kinetic barrier of decomposition reaction supports hypothesis of rock salt phase formation. Namely, Fm-3m

Table 2
Percentage mass losses (normalised to mass of $LiCoO_2$ in the sample) at 600 °C.

$LiCoO_2$ surface area	Pure $Li_{0.5}CoO_2$	Pure $Li_{0.5}CoO_2$ + acetylene black (8:1)	Pure $Li_{0.5}CoO_2$ + PVDF (8:1)	Charged cathode
0.4 m^2 g^{-1}	4.30%	7.20%	16.27%	15.90%
18.3 m^2 g^{-1}	8.10%	11.19%	19.79%	21.14%
42.4 m^2 g^{-1}	13.84%	16.40%	23.12%	23.39%

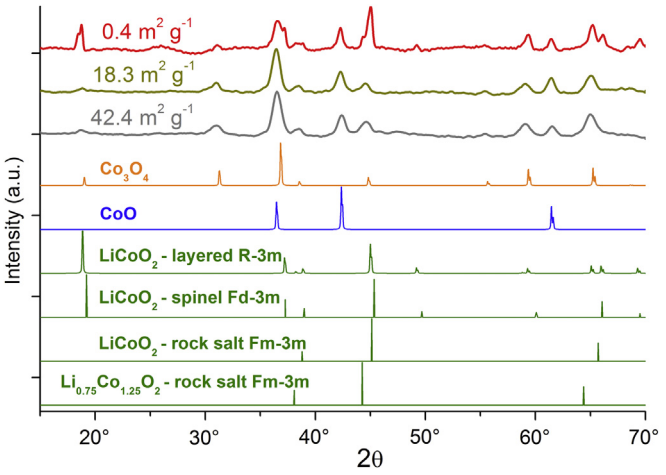

Fig. 7. XRD spectra of decomposed cathodes (heated up to 600 °C) compared to standards for $LiCoO_2$ (layered, spinel and rock salt), Co_3O_4 and CoO. Absence of layered $LiCoO_2$-related peaks is obvious for the two cathodes with higher surface area.

$Li_yCo_{2-y}O_2$ is thermodynamically stable only for $0 \leq y \leq 0.4$ if synthesized by thermal annealing [17]. Higher values of y would yield a layered R-3m structure. If there are in fact both bulk and surface reactions occurring and surface tends to be less stable, the activation energy of the overall reaction of cathode decomposition is expected to be lower. In addition to the hypothesis of different decomposition reactions in bulk and at surface (as elaborated in previous chapter), this explains how even at higher values of y ($y > 0.66$ as suggested in chapter 3.3), rock salt $Li_yCo_{2-y}O_2$ can be formed.

3.5. Thermal stability of cathode-electrolyte system

Further study of the thermal stability of the electrode was carried out by ARC. Fig. 9 shows the dependence of self-heating temperature rate vs. sample temperature for the system of charged cathode and electrolyte. The surface area of $LiCoO_2$ does not have significant impact on the onset temperature of spontaneous self-heating, which is about 300 °C for the three samples. This may be because the initially detected reaction is due to the auto ignition of the electrolyte. However, the surface area of the

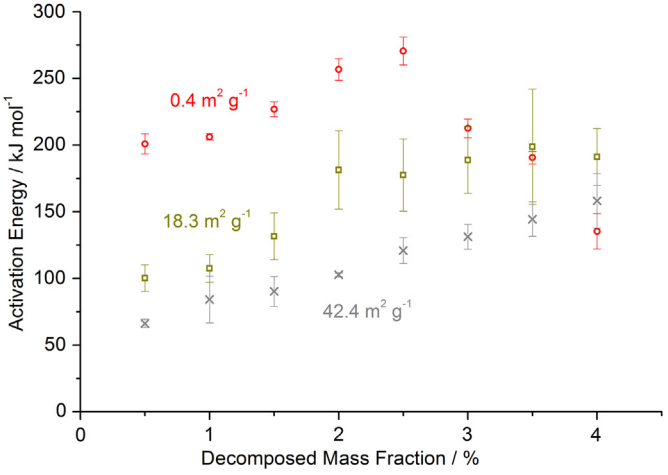

Fig. 8. Calculated Arrhenius activation energy at different values of conversion, expressed by decomposed mass fraction. Error bars are determined from goodness of fitting of the TGA data to equation (5).

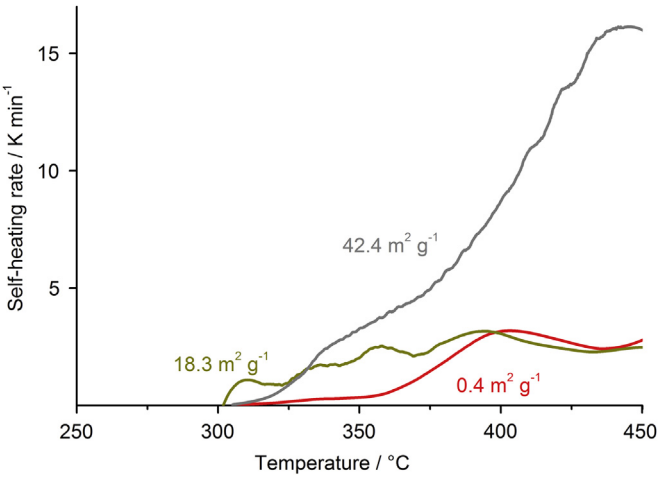

Fig. 9. ARC of charged cathodes with addition of 1 M $LiPF_6$ EC/DEC electrolyte in mass ratio 2:1.

active material has large influence on the self-heating rate of the reaction: The higher the surface area, the higher the heating rate. This is probably because of the larger surface area available for oxygen evolution and the increased amount of oxygen released from $Li_{0.5}CoO_2$ (as suggested in 3.3), which accelerate the reaction with electrolyte.

In ARC, the ratio between thermal mass of whole system (sample + holder) to thermal mass of reacting substance, also known as Phi-factor, affects the onset and rate [14]. Absence of a standard and consequent usage of self-made sample holders makes ARC results of different researchers hardly comparable. A high Phi-factor may lead to absorption of a large portion of released heat by sample holder. This is the reason why earlier cathode decomposition reactions in the sample, despite being exothermal, were undetected by ARC.

4. Conclusions

Thermal stability of $LiCoO_2$ cathode is highly dependent on surface area of the active material. Increasing the surface area by reducing particle size results in a lower decomposition onset temperature and a higher amount of mass loss. The amount of decomposed mass at 400 °C increases linearly with surface area.

Milled high surface $LiCoO_2$ decomposes differently compared to pristine, as-synthesized $LiCoO_2$. Higher mass loss implies that decomposition of high surface area $Li_{0.5}CoO_2$ releases more oxygen from the cathode. Phase composition of decomposition reaction products changes as well. Formation of $Li_yCo_{2-y}O_2$ with rock salt (Fm-3m) structure upon decomposition of high surface area $Li_{0.5}CoO_2$ is hypothesized. This can be explained by different decomposition reactions at surface and in bulk of active material. Further research is underway to explain this phenomenon.

Calculated Arrhenius activation energy at different stages of conversion implies that charged cathode with high-surface $LiCoO_2$ has lower kinetic barrier for decomposition. More favourable kinetics also supports the claim of formation of allegedly thermodynamically less stable rock salt structure in place of layered $LiCoO_2$.

Cathode-electrolyte system is less stable if $LiCoO_2$ has a higher surface area. Ignition-induced self-heating rate is higher in such case. The reasons are higher oxygen content available from decomposition of high surface cathode and better contact between evolving oxygen and electrolyte due to high surface area.

The results presented in this paper show that decreasing the particle size of $LiCoO_2$ by ball milling considerably reduces thermal stability of charged $LiCoO_2$ cathodes, mainly due to increase of surface area and possibly due to crystal structure and/or surface defects. Milling should therefore be avoided for preparing $LiCoO_2$ active material for lithium ion cathodes.

Acknowledgements

This work was financially supported by the Singapore National Research Foundation under its Campus for Research Excellence and Technological Enterprise (CREATE) programme.

The authors are thankful to Ms Yin Ting Teng from Energy Research Institute at Nanyang Technological University in Singapore for her technical support with X-ray diffraction spectroscopy.

References

[1] H. Awano, in: M. Yoshio (Ed.), Lithium-Ion Batteries, Science and Technology, Springer Science + Business Media LLC, 2009, pp. 300–301.
[2] P.G. Bruce, B. Scrosati, J.-M. Tarascon, Angew. Chem. Int. Ed. 47 (2008) 2930–2946.
[3] M. Jo, Y.-S. Hong, J. Choo, J. Cho, J. Electrochem. Soc. 156 (2009) A430–A434.
[4] M. Jo, S. Jeong, J. Cho, Electrochem. Comm. 12 (2010) 992–995.
[5] N.N. Sinha, N. Munichandraiah, J. Indian Inst. Sci. 89 (2009) 381–392.
[6] Y. Furushima, C. Yanagisawa, T. Nakagawa, Y. Aoki, N. Muraki, J. Power Sources 196 (2011) 2260–2263.
[7] A. Veluchamy, C.-H. Doh, D.-H. Kim, J.-H. Lee, H.-M. Shi, B.-S. Jin, H.-S. Kim, S.-I. Moon, J. Power Sources 189 (2009) 855–858.
[8] J. Jiang, J.R. Dahn, Electrochim. Acta 49 (2004) 2661–2666.
[9] O.A. Shlyakhtin, S.H. Choi, Y.S. Yoon, Y.-J. Oh, Electrochim. Acta 50 (2004) 511–516.
[10] T. Ozawa, Bull. Chem. Soc. Jpn. 38 (1965) 1881–1886.
[11] S. Vyazovkin, Int. J. Chem. Kinet. 28 (1996) 95–101.
[12] K. Nakamura, H. Hirano, D. Nishioka, Y. Michihiro, T. Moriga, Solid State Ionics 179 (2008) 1806–1809.
[13] S. Kinzy, R. Falcone, in: H. Lobo, J.V. Bonilla (Eds.), Handbook of Plastics Analysis, CRC Press, 2003, p. 126.
[14] D.I. Townsend, J.C. Tou, Thermochim. Acta 37 (1980) 1–30.
[15] M. Okubo, E. Hosono, J. Kim, M. Enomoto, N. Kojima, T. Kudo, H. Zhou, I. Honma, J. Am. Chem. Soc. 129 (2007) 7444–7452.
[16] M. Antaya, K. Cearns, J.S. Preston, J.N. Reimers, J.R. Dahn, J. Appl. Phys. 76 (1994) 2779–2806.
[17] W.D. Johnston, R.R. Heikes, D. Sestrich, J. Phys. Chem. Solids 7 (1958) 1–13.
[18] M.N. Obrovac, O. Mao, J.R. Dahn, Solid State Ionics 112 (1998) 9–19.